Title

Partial Observability Analysis of an Adversarial Swarm Model

Journal

Journal of Guidance Control and Dynamics, 43(2)

ISSN

0731-5090

Authors

Gong, Qi
Kang, Wei
Walton, Claire
et al.

Publication Date

2020-02-01

DOI

10.2514/1.g004115

Peer reviewed

Partial Observability Analysis of an Adversarial Swarm Model

Qi Gong *
University of California, Santa Cruz, CA 95064

Wei Kang † Claire Walton ‡ and Isaac Kaminer §
Naval Postgraduate School, Monterey, CA 93940

Hyeongjun Park¶
New Mexico State University, Las Cruces, NM 88003

This paper introduces a new concept of partial observability for nonlinear systems. This new approach enables a quantitative analysis on the observability of an individual state variable and unknown parameters of a nonlinear dynamics even when the system is not observable in the traditional sense. The paper develops theoretical properties of partial observability and its computational algorithms. These results are applied and validated on a non-standard estimation problem of detecting the internal cooperating strategy of a particular adversarial swarm model. Partial observability analysis on the parameters that define the cooperating strategy reveals interesting findings. For example, some parameters are observable even when the swarm is at a steady state that is not observable in traditional sense. It is also shown that observability of the internal cooperating strategy depends on both the swarm trajectory and the time window of the measurement. Motivated by these findings, a variational method of estimation based on the dynamic optimization of a cost function is proposed. Simulation results show that the proposed estimation method outperforms Kalman filters. The results in this paper provide useful tools for applications involving adversarial swarms, including defense against swarm attacks and herding of biological swarms.

I. Introduction

In the past few decades, the research community has produced multiple models for simulating swarm behavior, such as those developed by Leonard *et al*. at Princeton University [1, 2], Jadbabaie *et al*. [3], and Szwaykowska *et al*. at Naval Research Laboratory [4], and methods for implementing autonomous swarms, such as the autonomous swarms being flown by Chung *et al*. at Naval Postgraduate School [5]. The aforementioned models and methods consider challenges related to autonomous swarms from what could be termed an *insider's perspective*–that is, from the perspective of

*Professor, Department of Applied Mathematics, qigong@soe.ucsc.edu.
†Professor, Department of Applied Mathematics, wkang@nps.edu
‡Research Associate, Department of Mechanical and Aerospace Engineering, cwalton1@nps.edu
§Professor, Department of Mechanical and Aerospace Engineering, kaminer@nps.edu
¶Assistant Professor, Department of Mechanical and Aerospace Engineering, hjpark@nmsu.edu

creating, controlling, and driving one's own autonomous or semi-autonomous swarm.

As applications of autonomous swarms become more widespread, how to analyze interactions with swarms emerges as an important research topic. Swarms may be indirectly adversarial—conflicting with objectives simply due to not being under our control, as would be the case interacting with a natural swarm such as a bird flock, or with an outside team of vehicles. Or these swarms may be directly adversarial, in competition or conflict with our goals, as will be faced in defense scenarios. An example of a goal action against an adversarial swarm is herding—guiding or containing a group through interaction with their innate reactive mechanisms. In [6] for instance, an aerial robot is used to guide a flock of birds away from a protected airspace. Another example is defense against attacks from an adversarial swarm. In [7], multi-vehicle trajectory optimization for defense of an asset against an oncoming swarm of autonomous vehicles is considered.

In both these applications, identifying a model of an adversarial swarm is essential. Swarms' internal control strategies such as collision avoidance distances, swarm cohesion, and communication distances determine swarm behaviors and their responses to external disturbances. Without a pre-established swarm model, these strategies must be estimated through observation and/or interaction of the swarm. For example, in Ref. [6] where the problem of herding of a flock of birds was considered, the parameter of collision avoidance distance that defines the flock dynamics was estimated using real experimental data.

In this paper we address the problem of detecting the internal cooperating strategy of a particular adversarial swarm whose dynamics is subject to the swarm model developed by Leonard *et al*. [1, 2]. This swarm model is based on a potential function and virtual leaders, which can be characterized by a set of parameters. Thus, by estimating those parameters one can identify the internal cooperating strategy of an adversarial swarm. Note that, this is a nonstandard estimation problem—the estimation problem we address in this paper is not to estimate, for example, position and velocity of each member of the swarm; rather we are interested in understanding how individual agents cooperate to achieve the swarm behavior that is observed by outsiders.

Prior to actually designing an estimator a natural question is whether these parameters are in fact *observable*, i.e., can be successfully estimated from the sensor measurement. The observability is an intrinsic property of a dynamical system with sensor information and user-knowledge. It defines the essential limitation in estimation and detection. The literature on observability analysis and observer design is quite extensive, see for example [8–13]. However, the classical observability analysis tools, including the rank conditions [8, 9], do not apply to the observability analysis of an adversarial swarm cooperating strategy due to nonlinearities and discontinuities inherent in the model. In our previous work [14], the concepts of unobservability index and empirical observability Gramian [15–17] were utilized to analyze the observability of a potential function based swarm modeled developed in [1, 2]. It is shown in [14] that the steady state of the swarm is *unobservable*. To make the system observable, Ref. [14] proposes to use intruders as a possible agent provocateur disrupting the adversarial swarm and provoking the swarm into more revealing behaviors. While

intruder perturbations make the system observable, the simulations in [14] also reveal that standard filtering techniques such as unscented Kalman filter (UKF) often fail to estimate the parameters that define the internal cooperating strategy. The failure of standard estimation algorithms can be attributed to the parameters in the swarm model that represent the range limit of communication and/or range of influence among agents. These parameters introduce discontinuity into the swarm dynamics. In the state-parameter space, they are observable in a zero measure set within a short time interval only, making the design of a convergent estimation algorithm very challenging.

In this paper, in contrast to [14], we introduce a new tool of partial observability to study the observability of any variable of interest in a nonlinear system. This new concept enables quantitative observability analysis for an individual state variable even when the system is *unobservable* in traditional sense. We derive theoretical results that reveal properties of partial observability, and link it to other observability metrics. As a particular attractive feature, partial observability can be conveniently computed using empirical observability Gramian and optimization, making it suitable for analyzing complex nonlinear systems such as a swarm of autonomous agents. When applied to the swarm model studied in [1, 2, 14], partial observability analysis reveals that, even at steady state when the system is not observable in traditional sense as shown in [14], some parameters in the cooperating strategy are still observable and can be successfully estimated. Moreover, in the presence of intruders, our analysis shows the dependence of observability on the time window of the sensor measurements. Such feature imposes a fundamental challenge on Kalman filter type of sequential estimation techniques.

To address such issues in estimating parameters in an adversarial swarm, we propose a two-step dynamical optimization based method that processes the measurement in a batch fashion. The algorithm leverages on the results obtained by partial observability analysis to improve the computational efficiency. It also resolves the challenge of estimating parameters that are only observable on a zero measure set. As the number of agents increases, computational cost of the proposed two-step estimation algorithm also grows rapidly. Thus, the algorithm is most suitable for small size swarms. Estimation of large swarms is an interesting topic for future research.

This paper is organized as follows. In Section II we define the concept of partial observability for nonlinear systems; prove some fundamental properties; and develop computational tools for analyzing partial observability. These concepts and tools are applied in Section III on an adversarial swarm model to analyze the observability of internal swarm cooperating strategies. Two baseline scenarios are studied in detail. One is when the swarm is at a steady state, the other addresses the case when the swarm is perturbed by intruders. Based on the partial observability analysis, we propose a two-step estimation algorithm in Section IV; and compare its performance with that of an UKF. Finally, some concluding remarks are given in Section V.

II. Partial Observability

In this section, we develop the theoretical foundation and a computational method for the partial observability of nonlinear systems. In Part A, we introduce the concept of partial observability defined in [18]. The concept is closely related to the observability Gramian in the linear control theory. In Part B, we develop a new method of computing the partial observability of linear systems based on the optimization of a quadratic function and observability Gramian. It is proved that the unobservability index concides with the Lagrangian multiplier of the optimization. Necessary and sufficient conditions for the boundedness of unobservability index are proved. If the system is nonlinear, its unobservability index is approximated using an empirical Gramian along a nominal trajectory. The method developed in this section is different from existing literature on this topic [15, 16] in which either the full observability is computed or a more complicated optimization problem with dynamic constraints must be solved. In Part C, we provide a computational approach by introducing the norms and their weighting matrices for a family of nonlinear problems that include the swarm examples studied in this paper.

A. Concepts and definitions

Consider a control system

$$\begin{aligned} \dot{x} &= f(t, x, u, p), \quad x \in \mathbb{R}^{n_x}, u \in \mathbb{R}^{n_u}, p \in \mathbb{R}^{n_p} \\ y &= h(t, x, u, p), \qquad\qquad\qquad\quad y \in \mathbb{R}^{n_y}. \end{aligned}$$

where x is the state variable, u is the control input, p represents the constant vector of parameters. The variable y is the output of the system, which can be measured using sensors. The time interval is $[t_0, t_f]$. Although differential equations are widely used as mathematical models of control systems, real-life operations are often subject to additional constraints. For instance, the following is a list of some examples

$E(x(t_0), x(t_f)) \le 0,$	end-point condition
$s(x(t), u(t)) \le 0, \ \forall t \in [t_0, t_f],$	state-control constraints
$p_1 \le p \le p_2,$	model uncertainty
$d(x(t), p) = 0, \ \forall t \in [t_0, t_f],$	differential-algebraic equations
$u = u(t),$	known control input, an assumption often used in control theory

These additional constraints represent known information, or user-knowledge, about the system. In general, user-knowledge helps to improve observability. It is modeled as a subset in the space of state-control trajectories

$$(x(\cdot), u(\cdot), p) \in C$$

In partial observability, the goal is to estimate the projection of the state variable into a subspace. The variable to be estimated is denoted by z. It is modeled using a mapping, or projection $\mathcal{P}$,

$$z = \mathcal{P}(x(\cdot), u(\cdot), p).$$

For example, if we want to estimate $x_1(0)$ only, then $\mathcal{P}(x(\cdot), u(\cdot), p) = x_1(0)$. We would like to point out that the definition of observability does not require a known control input, i.e., the value of $u(t)$ can be unknown. In the study of non-cooperative systems, the control input is not necessarily given or measurable. The entire system model is summarized as follows

$$\dot{x} = f(t, x, u, p), \qquad x \in \mathbb{R}^{n_x}, u \in \mathbb{R}^{n_u}, p \in \mathbb{R}^{n_p} \tag{1a}$$

$$(x(\cdot), u(\cdot), p) \in C \tag{1b}$$

$$y = h(t, x, u, p), \qquad y \in \mathbb{R}^{n_y} \tag{1c}$$

$$z = \mathcal{P}(x(\cdot), u(\cdot), p), \qquad z \in \mathbb{R}^{n_z} \tag{1d}$$

We assume that trajectories, as functions of t, have a norm in L^2 space. The metrics used for x, y, and z are denoted by $||\cdot||_X$, $||\cdot||_Y$ and $||\cdot||_Z$, respectively. Let $(x(t), u(t).p)$, $t \in [t_0, f_f]$ be a nominal trajectory around which we study the system's observability. For nonlinear systems, changing the nominal trajectory or the time window may result in the change of the observability. Therefore, the observability computed for a nominal trajectory is valid only in a region around the nominal trajectory. Let $\epsilon > 0$ be a small number. The set, $\mathcal{E}$, of trajectories is defined as follows

$$\mathcal{E} = \{(\hat{x}(\cdot), \hat{u}(\cdot), \hat{p})| \text{ it satisfies (1a)-(1b) and } ||\hat{y}(\cdot) - y(\cdot)||_Y \leq \epsilon\} \tag{2}$$

where $\hat{y}(\cdot)$ is the output of $(\hat{x}(\cdot), \hat{u}(\cdot), \hat{p})$ and $y(\cdot)$ is the output of the nominal trajectory. If ϵ represents the upper bound of sensor error, then the trajectories in $\mathcal{E}$ are all similar to the nominal trajectory in the sense that they are indistinguishable based on sensor data and user-knowledge. Therefore, the size of $\mathcal{E}$ determines the observability of the nominal trajectory. The observability of z is determined by the size of the set $\mathcal{P}(\mathcal{E})$. If this set is small, it means that the ambiguity in the estimation of z is small, i.e., z is observable.

Definition 1 *Let ρ be a metric that measures the size of $\mathcal{P}(\mathcal{E})$, then ρ is a measure of unobservability of z. It is called the estimation ambiguity.*

There are different ways to measure the size of a set. In this paper, we use the radius as a metric.

Definition 2 *The radius of $\mathcal{E}$, also a measure of estimation ambiguity, is defined as follows*

$$\rho = \max_{(\hat{x}(\cdot),\hat{u}(\cdot),\hat{p})\in\mathcal{E}} ||\mathcal{P}(t,\hat{x}(\cdot),\hat{u}(\cdot),\hat{p}) - \mathcal{P}(t,x(\cdot),u(\cdot),p)||_Z \tag{3}$$

where $||\cdot||_Z$ is the Euclidean norm if z is a vector and L^2-norm if z is a function. The ratio ρ/ϵ is called the unobservability index

Unobservability index quantifies the observability of a nonlinear system. A small unobservability index implies strong observability of the system. The concept of unobservability index has been used in the literature for various applications [15, 16, 19].

B. A linear perspective

This definition of observability is consistent with that in the classical control theory of linear systems. Consider

$$\begin{aligned} \dot{x} &= Ax, \qquad t \in [0,T] \\ y &= Cx, \\ z &= x(0). \end{aligned} \tag{4}$$

where $x \in \mathbb{R}^{n_x}$ is the state variable and $y \in \mathbb{R}^{n_y}$ is the output variable. Let's consider the observability of the initial state, $z = x(0)$. Thus $n_x = n_z$ and the mapping in (1d) is a simple projection

$$\mathcal{P}(x(\cdot)) = x(0)$$

In the linear control theory, the observability is determined by an observability Gramian, which is a non-negative symmetric matrix

$$G = \int_0^T e^{A^T\tau} C^T C e^{A\tau} d\tau \geq 0.$$

In this case, the unobservability index is equivalent to the smallest eigenvalue of the observability Gramian as shown in the following result. Its proof is given in the Appendix.

Propostion 1 *([18]) Consider the observability of z in the linear system (4). Let G be the observability Gramian. Given $\epsilon > 0$. Let $\lambda_{\min}$ and $x_{\min}$ be the smallest eigenvalue and its associate eigenvector satisfying $\lambda_{\min}||x_{\min}||_2^2 = \epsilon^2$. Then, $\mathcal{P}(\mathcal{E})$ is the following ellipsoid*

$$\mathcal{P}(\mathcal{E}) = \left\{ x(0) + \delta x(0) \,\middle|\, \delta x(0)^T G \delta x(0) \leq \epsilon^2 \right\} \tag{5}$$

The estimation ambiguity, i.e., the radius of the ellipsoid, is $\rho = ||x_{\min}||_2$. *The unobservability index equals* $\rho/\epsilon = 1/\sqrt{\lambda_{\min}}$.

In general, the "size" of an ellipsoid can be measured using different metrics, such as the determinant of G, the trace of G, or the condition number of G. In [20], a comparison of various quantitative measures of observability is studied for power systems. For linear systems with sensor noise that follows a normal distribution, the observability Gramian coincides with the Fisher information matrix of the output function with respect to the initial state.

For partial observability, let's consider a special case where $z = Px(0)$. Matrix P is of dimension n_z by n_x, with $n_z < n_x$. The mapping in (1d) is a projection to subspace

$$\mathcal{P}(x(\cdot)) = Px(0)$$

and

$$\mathcal{P}(\mathcal{E}) = \{Px(0) + P\delta x(0) | \delta x(0)^T G \delta x(0) \leq \epsilon^2\}$$

The radius of this set, or the estimation ambiguity (3), is equivalent to the following constrained maximization

$$\begin{aligned} \rho^2 = &\max_{x \in \mathbb{R}^n} \{\|Px\|^2\} \\ &\text{Subject to} \\ &x^T G x = \epsilon^2 \end{aligned} \tag{6}$$

Define the Lagrangian function for solving (6),

$$L = x^T P^T P x - \lambda x^T G x$$

where $\lambda \in \mathbb{R}$ is the Lagrange multiplier. Then the maximization in (6) is achieved at points satisfying the following necessary conditions

$$\begin{aligned} P^T P x &= \lambda G x \\ x^T G x &= \epsilon^2 \end{aligned} \tag{7}$$

Propostion 2 *The estimation ambiguity of* $z = Px(0)$ *is the largest value of* $\rho = \|Px^*\|_2$ *among all pairs* (x^*, λ^*) *that satisfy (7). The corresponding value of the Lagrange multiplier,* λ^**, equals the square of the unobservability index.*

Proof: The necessary condition (7) is obvious. If (x^*, λ^*) maximizes ρ, multiply $(x^*)^T$ to the first equation in (7), we have

$$\|Px^*\|_2^2 = \lambda^* (x^*)^T G x^*.$$

Because $\rho^2 = \|Px^*\|_2^2$ and $(x^*)^T G x^* = \epsilon^2$, we have

$$\lambda^* = \rho^2/\epsilon^2$$

i.e. the square of the unobservability index equals the Lagrange multiplier. □

Proposition 2 links the concept of partial unobservability index to the Lagrange multiplier of the optimization problem (7). It is not surprising, since the Lagrange multiplier measures the sensitivity of the cost function to the variations of initial states. The following result establishes a sufficient condition under which the optimization problem (7) is well defined.

Propostion 3 *Consider optimization problem (7). Let $Nul(G)$ and $Nul(P)$ be the null space of G and P respectively.*

1) If $Nul(G) \subseteq Nul(P)$, the unobservability index of $z = P(x(0))$ is finite.

2) If $Nul(G)$ is not a subset of $Nul(P)$, the unobservability index of $z = Px(0)$ is ∞, i.e., z is unobservable.

Proof: Let $r \leq n_x$ be the rank of the positive semi-definite matrix G, and denote the singular values of G as

$$\sigma_1 \geq \sigma_2 \geq \cdots \geq \sigma_r > 0.$$

Consider the singular value decomposition $G = U\Sigma U^T$, where U is an orthogonal matrix and $\Sigma = diag(\sigma_1, \ldots, \sigma_r, 0, \ldots, 0)$ is a diagonal matrix. Then, the null space of G is given by

$$Nul(G) = span\{u_{r+1}, u_{r+2}, \ldots, u_n\},$$

where u_i is the ith column of U. For all $x \in R^n$ satisfying $x^T G x = \epsilon^2$, let $\bar{x} = U^T x$. We have

$$x^T G x \;=\; \bar{x}^T U^T G U \bar{x} \;=\; \bar{x}^T \Sigma \bar{x} \;=\; \sigma_1 \bar{x}_1^2 + \sigma_2 \bar{x}_2^2 + \cdots + \sigma_r \bar{x}_r^2 = \epsilon^2, \tag{8}$$

where $\bar{x}_i$ is the i-th entry of vector $\bar{x}$. If $Nul(G) = span\{u_{r+1}, u_{r+2}, \ldots, u_n\} \subseteq Nul(P)$,

$$\begin{aligned} Px &= PU\bar{x} = [Pu_1, \ldots, Pu_r, 0, \ldots, 0]\bar{x} \\ &= \bar{x}_1 Pu_1 + \cdots + \bar{x}_r Pu_r. \end{aligned}$$

Therefore,

$$\|Px\|_2 \;\leq\; |\bar{x}_1| \cdot \|Pu_1\| + \cdots + |\bar{x}_r| \cdot \|Pu_r\|$$

where the right hand side must be bounded because of (8) and the fact that $\sigma_i > 0$ for all $i \leq r$.

If $Nul(G)$ is not a subset of $Nul(P)$, there is a vector $v \in Nul(G)$ such that $Gv = 0$ and $Pv \neq 0$. Let x be an arbitrary vector satisfying $x^T Gx = \epsilon^2$. Then

$$(x+v)^T G(x+v) \quad = \quad x^T Gx \; = \; \epsilon^2.$$

Therefore, $x + v$ satisfies constraint in (6). The corresponding cost is $\|P(x+v)\|_2^2 = \|Px + Pv\|_2^2$, which can be arbitrarily large, since $Pv \neq 0$ and v can be scaled to have an arbitrarily large length. Hence, $\rho/\epsilon = \infty$. □

In traditional control theory, observability is analyzed with respect to initial condition $x(0)$, i.e., $P = I$. If G has rank deficiencies, $Nul(G)$ is clearly not a subspace of $Nul(P)$. Based on Proposition 3, ρ is infinity and $x(0)$ is not observable, which is consistent to classical observability theory. However, even for the case when G is not full rank, user-knowledge, such as the bounds of state variables, can be applied to still find a finite value of estimation ambiguity. In this case, a set of lower and upper bounds to x is added to the constraints of the maximization problem (6),

$$\begin{aligned} \rho^2 \quad &= \max_{x \in \mathbb{R}^n} \{\|Px\|^2\} \\ \text{Subject to} \quad & x^T Gx = \epsilon^2 \\ & m_i \leq x_i \leq M_i, \quad \text{for } i = 1, 2, \cdots, n_x \end{aligned} \tag{9}$$

where m_i and M_i are constants representing users knowledge on the state variables.

C. Computational implementation

The general definition of observability is equivalent to a problem of constrained dynamical optimization (3). For linear systems, by using observability Gramian, optimization problem (3) can be reduced to a finite dimensional optimization (6), which can be easily solved to obtain partial unobservability index. For nonlinear systems, one is unlikely to get an analytic solution for the nonlinear dynamic optimization (3). In this paper we adopt the concept of empirical Gramian to approximate nonlinear dynamic optimization (3) by a finite dimensional optimization problem. As a first order approximation, empirical Gramian was used to approximate the unobservability index in [15, 16, 19] for nonlinear systems. The empirical observability Gramian is defined using the original nonlinear dynamics along a nominal trajectory. It reflects the observability of the full nonlinear system in a region along the nominal trajectory. This is in sharp contrast to a traditional approach based on linearization of the system around an operating point.

Consider a control system

$$\dot{x} = f(t, x, u, p), \qquad x \in \mathbb{R}^{n_x}, u \in \mathbb{R}^{n_u}, p \in \mathbb{R}^{n_p} \tag{10a}$$

$$y = h(t, x, u, p), \qquad y \in \mathbb{R}^{n_y} \tag{10b}$$

$$z = [x_1(0), \cdots x_{n_z}(0)]^T, \qquad z \in \mathbb{R}^{n_z} \tag{10c}$$

The individual state variables in a system may use different units. Their estimation error tolerances are different. Therefore we need a weighted norm as the metric of z. Let the error tolerance in the estimation of z be a set of positive numbers $\delta_1, \delta_2, \cdots, \delta_{n_z}$ in their own units. Define an inner product using a diagonal matrix

$$W_Z = \text{diag}(1, \delta_1/\delta_2, \cdots, \delta_1/\delta_{n_z})$$
$$< z_1, z_2 >_Z = z_1^T W_Z^T W_Z z_2$$
$$||z||_Z = < z, z >_Z^{1/2}$$

This set of weights rescales z based on the error tolerance and the corresponding unit of z_1. The accuracy of estimation is justified by comparing the error to δ_1. A standard orthogonal basis consists of the column vectors of W_Z^{-1},

$$w_1 = e_1$$
$$w_i = \frac{\delta_i}{\delta_1} e_i, \quad i = 1, 2, \cdots, n_z$$

where e_i's are the column vectors of the identity matrix. Choose a small $\delta > 0$, consider

$$x^{\pm i}(0) = x(0) \pm \delta w_i, \quad i = 1, 2, \cdots, n_x$$

Let $y^{\pm i}(t)$ represents the corresponding output. To define a weighted inner product for y, one can use the sensor error covariance as the weight matrix. If sensor errors are not correlated, the matrix is diagonal. More specifically, suppose the sensor error standard deviations are $\sigma_1, \sigma_2, \cdots, \sigma_{n_y}$. For some sensors, we may use error upper bounds in a similar way. Similar to W_Z, we define

$$W_Y = \text{diag}(1, \sigma_1/\sigma_2, \cdots, \sigma_1/\sigma_{n_y})$$

The empirical Gramian at $x(0)$ is the $n \times n$ matrix G_Y whose (i, j)-component is defined as

$$\begin{aligned} \Delta_i(t) &= \frac{1}{2\delta}\left(y^{+i}(t) - y^{-i}(t)\right), \\ \left\langle \Delta_i, \Delta_j \right\rangle_Y &= \int_{t_0}^{t_f} \Delta_i(t)^T W_Y^T W_Y \Delta_j(t) dt \\ G &= \left(\left\langle \Delta_i, \Delta_j \right\rangle_Y\right)_{i,j=1}^{n_x}, \end{aligned} \tag{11}$$

Using (6) as a first order approximation of the estimation ambiguity, ρ is the solution of the following constrained maximization

$$\begin{aligned} \rho^2 &= \max_{x \in \mathbb{R}^n} \|W_Z z\|^2 \\ &\text{Subject to} \\ x^T G x &= \epsilon^2 \end{aligned} \tag{12}$$

The value of ρ can be interpreted as follows. If the sensor error is bounded by ϵ, under the weighted norm, then ρ is approximately the worst estimation error of a maximum likelihood estimator that is based on the difference of the output function and the sensor data. The ratio, ρ/ϵ, is approximately the unobservability index.

III. Observability Analysis of an Adversarial Swarm

In this section we apply the concept of partial observability introduced in the previous section on analyzing cooperation strategies in adversarial swarms. As an illustrative example, we consider an adversarial swarm governed by a dynamical model proposed by Leonard *et al*. [1]. The model consists of multiple agents including followers and virtual leaders. All agents are assumed as point masses in xy-plane with fully actuated dynamics.

$$\begin{aligned} \ddot{x}_{l_k} &= u_{l_k}, \;\; k = 1, \ldots, m, \\ \ddot{x}_i &= u_i. \;\; i = 1, \ldots, n, \end{aligned} \tag{13}$$

where $x_{l_k} \in \mathbb{R}^2$ and $u_{l_k} \in \mathbb{R}^2$ are position and input vectors of virtual leaders, $x_i \in \mathbb{R}^2$ and $u_i \in \mathbb{R}^2$ are position and input vectors of each agent, and m and n are the numbers of virtual leaders and followers. Fig. 1 illustrates a swarm with multiple vehicles and a virtual leader.

The interaction force between two agents has magnitude f_I and is a gradient of an artificial potential V_I. Both the artificial potential V_I and force f_I depend on the distance $||x_{ij}||$ between the vehicle i and its neighbor vehicle j. The

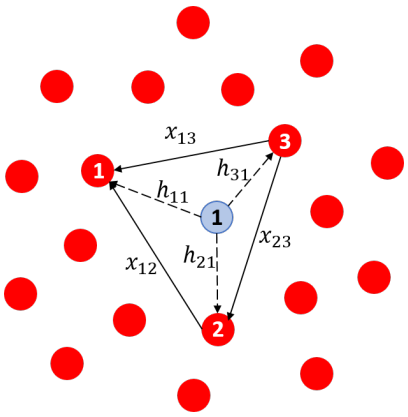

Fig. 1 Example of multiple agents (red circles) and a virtual leader (blue circle)

artificial potential V_I is assumed to be in the form ([1, 2])

$$V_I = \begin{cases} \alpha\left(\ln\left(||x_{ij}||\right) + \dfrac{d_0}{||x_{ij}||}\right), & 0 < ||x_{ij}|| < d_1 \\ \alpha\left(\ln(d_1) + \dfrac{d_0}{d_1}\right), & ||x_{ij}|| \geq d_1 \end{cases} \tag{14}$$

where α is a scalar control gain, d_0 and d_1 are scalar constants for distance ranges. Then the magnitude of interaction force is given by

$$f_I = \begin{cases} \nabla_{||x_{ij}||} V_I, & 0 < ||x_{ij}|| < d_1 \\ 0, & ||x_{ij}|| \geq d_1 \end{cases} \tag{15}$$

Similarly, a potential V_h on a given agent i associated with the virtual leader k is defined with the distance $||h_{ik}||$ between the agent i and virtual leader k.

A dissipative force $f_{v_i} = -K(\dot{x}_i - \frac{1}{m}\sum_{k=1}^{m} \dot{x}_{i_k})$ is employed to guarantee stability of the swarm system, where K is a positive constant. This dissipative force enables each agent to follow a desired velocity. The control law u_i for the vehicle i associated with m virtual leaders and p intruders is given by

$$\begin{aligned} u_i &= -\sum_{j\neq i}^{n} \nabla_{x_i} V_I(x_{ij}) - \sum_{k=1}^{m} \nabla_{x_i} V_h(h_{ik}) + f_{v_i} \\ &= -\sum_{j\neq i}^{n} \frac{f_I(x_{ij})}{||x_{ij}||} x_{ij} - \sum_{k=1}^{m} \frac{f_h(h_{ik})}{||h_{ik}||} h_{ik} - K\left(\dot{x}_i - \frac{1}{m}\sum_{k=1}^{m} \dot{x}_{l_k}\right). \end{aligned} \tag{16}$$

The cooperation strategy of an adversarial swarm with dynamics (13)-(16) is completely determined by the state (positions and velocities) of the virtual leaders, artificial potentials V_I, V_h, and the feedback gain K. The question of interest is to recover the unknown cooperation strategy from the measurement made on the adversarial swarm. In this section, we will formulate the problem based on the concept of partial observability introduced in the previous section;

and analyze the observability of cooperation strategy through a sequence of numerical studies.

In all simulations presented in this paper, we make the following assumptions.

1) The swarm consists of 5 followers and 1 virtual leader, i.e., $n = 5$ and $m = 1$. The virtual leader moves along a straight line with a constant velocity; thus its trajectory depends only on its initial position and initial velocity, which are unknown.
2) The artificial potentials V_I and V_h are identical. The values of the parameters that define the potential function are set to be $\alpha = 150$, $d_0 = 100$ m, $d_1 = 200$ m, and $K = 1$. Fig. 2 shows the interaction force magnitude with the chosen parameters. Note that those parameter values are used to simulate swarm trajectories; but they are assumed to be unknown.

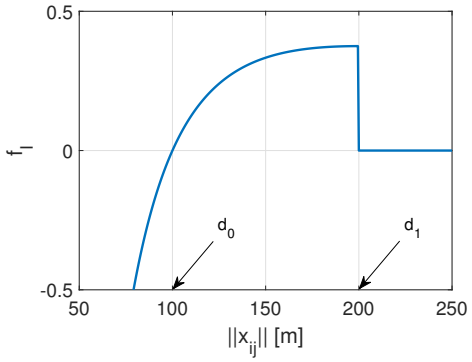

Fig. 2 Interaction force magnitude

3) All followers' states, i.e., position, $x_i(t)$, and velocity, $\dot{x}_i(t)$, $i = 1, \ldots, n$ are measurable.

The first assumption is the most restrictive one. Although the leaders' states are assumed to be unknown, we do require knowing the numbers of agents (followers and leaders) in an adversarial swarm. When this condition is not satisfied, the dimension of the dynamical system is unknown making the observability analysis a challenging problem. A possible approach is to perform observability analysis for a subgroup of a swarm, and design distributed estimation algorithms. It is an important topic of future research and out of the scope of this paper.

Under these assumptions, the problem of identifying the cooperation strategy is reduced to the problem of estimating initial virtual leader state, $(x_I(t_0), \dot{x}_I(t_0))$, and parameters α, d_0, d_1, and K, This problem is harder than it sounds. From an outsider's perspective, we do not have all the information like a controller. In fact, the overall system is unobservable in conventional control theory as shown in [14]. The parameters can be partially observable; or some are observable only on a zero measure set which makes Kalman filters fail to converge.

A. Partial observability analysis — steady state

For nonlinear systems, as explained in Section II, observability depends on the nominal trajectory. We first analyze the observability of a baseline scenario, where the adversarial swarm is at a steady state moving at a constant speed as

the virtual leader. The initial conditions of the swarm are given in Table 1, and illustrated in Fig. 3. Snapshots of the

Table 1 Initial positions and velocities of the followers and the leader.

Agent	Initial Position (m)	Initial Velocity (m/s)
virtual leader	$(0, 0)$	$(10, 0)$
follower 1	$(0.0003, 79.21)$	$(10, 0)$
follower 2	$(75.33, 24.48)$	$(10, 0)$
follower 3	$(46.56, -64.08)$	$(10, 0)$
follower 4	$(-46.56, -64.08)$	$(10, 0)$
follower 5	$(-75.33, 24.48)$	$(10, 0)$

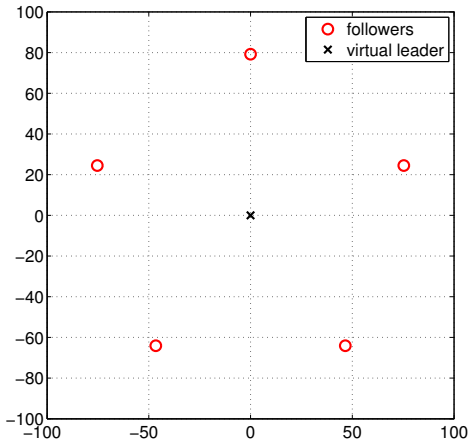

Fig. 3 Initial formation of the adversarial swarm.

motion of the swarm are shown in Fig. 4.

To study the partial observability of the considered adversarial swarm, we first use the computation method presented in Section II-C to calculate the empirical Gramian matrix, G, with the dynamics $\dot{x} = f(t, x, p)$ defined in (13)-(16), where the state is

$$x(t) = [x_l^T(t), \dot{x}_l^T(t), x_1^T(t), \dot{x}_1^T(t), \cdots, x_5^T(t), \dot{x}_5^T(t)]^T \in R^{24},$$

and the parameter is $p = [\alpha, d_0, d_1, K]$. The output is all followers' state, i.e.,

$$y(t) = [x_1^T(t), \dot{x}_1^T(t), \cdots, x_5^T(t), \dot{x}_5^T(t)]^T \in R^{20},\ t \in [0, 100]. \tag{17}$$

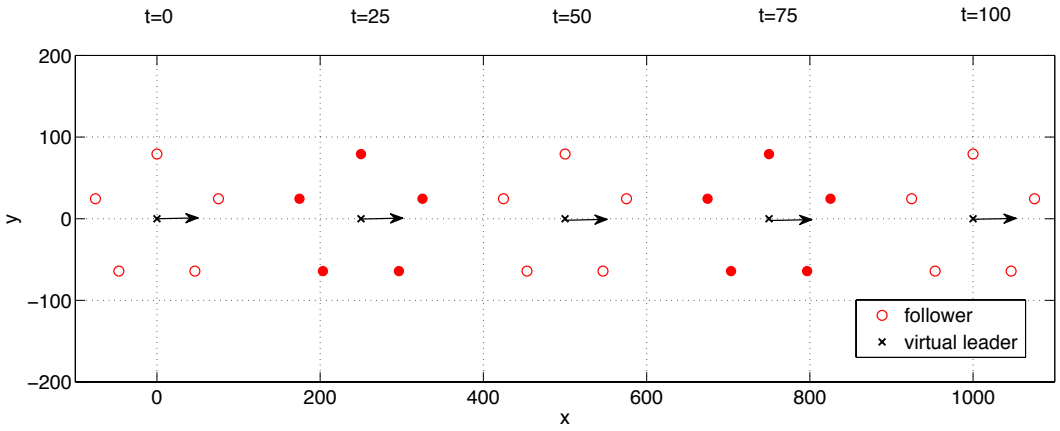

Fig. 4 Steady state motion of the adversarial swarm.

To compute the empirical observability Gramian matrix, the following perturbation is introduced

$$\begin{aligned} x^{\pm i}(0) &= x^{nom}(0) \pm \delta \cdot W_x E_x(i),\ i = 1, 2, \ldots, 24 \\ p^{\pm i} &= p^{nom} \pm \delta \cdot W_p E_p(i),\ i = 1, \ldots, 4, \end{aligned}$$

where $x^{nom}(0)$ is the initial condition of the nominal trajectory (steady state) and

$$p^{nom} = [150, 100, 200, 1]^T$$

is the nominal value of the parameters α, d_0, d_1 and K. $E_x(i)$ and $E_p(i)$ define the direction of the perturbations. In the simulation they are set to be the i-th column of the identity matrices of appropriate dimensions. In simulations the size of the perturbation is set at $\delta = 10^{-7}$. The weight matrix, W_x, is a block diagonal matrix with 6 (5 followers plus 1 leader) identical blocks. Each block is a diagonal matrix, $diag\,(1, 1, 0.1, 0.1)$. The parameter weight matrix, W_p is set to be a diagonal matrix of $diag\,(15, 10, 20, 0.1)$. Each perturbed initial conditions and parameters are propagated through the swarm dynamics for 100s to generate perturbed output trajectory

$$y^{\pm i}(t),\ i = 1, 2, \ldots, 28.$$

The empirical local observability Gramian is 24×24 matrix G whose (i, j) components is

$$\begin{aligned} \Delta_i(t) &= \frac{1}{2\delta} W_y (y^{+i}(t) - y^{-i}(t)),\ i = 1, \ldots, 28 \\ G_{i,j} &= \int_0^{100} \Delta_i(t)^T \Delta_j(t) dt, \end{aligned} \tag{18}$$

where weight matrix W_y is a block diagonal matrix with 5 identical blocks. Each block is a diagonal matrix $diag\,(1, 1, 10, 10)$.

The minimum eigenvalue of the computed empirical observability Gramian is 0, which implies that the unobservability index is $+\infty$ when z, the variable to be estimated, includes all state variables and all unknown parameters. In other words, the parameters of coordinating controller around the nominal trajectory (steady state) is not observable in the classical sense. The same conclusion was reported in our previous work [14]. Using the concept of partial observability, however, we can now further analyze the observability of individual variables of interest even when the whole system itself is not observable. Such analysis reveals more insights of a dynamical system than binary conclusion (fully observable or fully unobservable) obtained using methods like the one reported in [14].

Based on the computed empirical observability Gramian, the optimization problem (12) can be formulated and solved numerically. The results for individual parameters are shown in Table 2. From the results it is clear that leader

Table 2 Partial unobservability index of the steady state.

Estimation Variable (z)	Unobservability Index (ρ/ϵ)
Leader Position	1.779×10^{-1}
Leader Velocity	1.698×10^{-2}
Parameter α	$9.640 \times 10^{+3}$
Parameter d_0	6.208×10^{-3}
Parameter d_1	$2.000 \times 10^{+4}$
Parameter K	$1.000 \times 10^{+2}$

position, leader velocity, and parameter d_0 are all observable, while parameters α, d_1, and K are not. Intuitively, since the swarm is moving at a steady state, it is not surprising that virtual leader's velocity is observable, since they are the same as the followers' velocities. Our analysis shows that virtual leader's initial position and a part of the cooperation strategy, i.e., parameter d_0, are also observable. Such insight revealed based on partial observability analysis is not obvious from the physics of the dynamics. Different from the classical observability analysis, where only binary conclusion of the entire system can be obtained, the proposed partial observability analysis provides quantitive and component-wise evaluation.

As a mean to validate our partial observability analysis results, we apply UKF [21] on the steady state trajectory to estimate the unknown leader state and cooperation parameters $p = [\alpha, d_0, d_1, K]$. The results from a set of random UKF initial conditions are shown in Fig. 5-6. It is clear that UKF correctly identifies the leader state (position and velocity) and parameter d_0. However, the estimations for unobservable parameters, α, d_1 and K, do not converge.

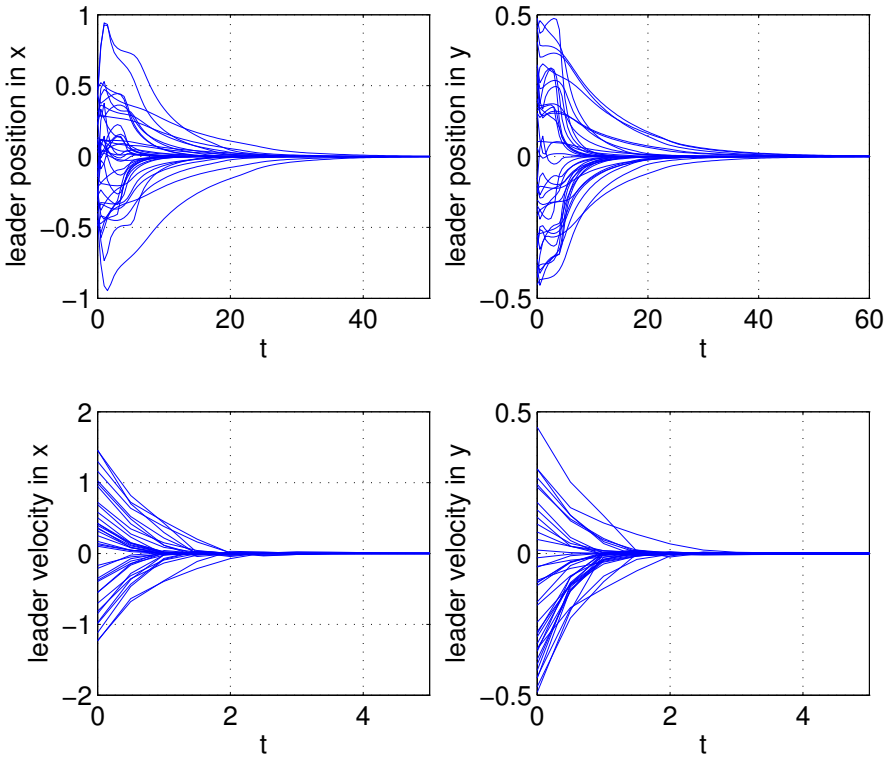

Fig. 5 UKF estimation errors of the leader state.

B. Partial observability analysis — intruder perturbation

We have shown that when a swarm has stabilized at an equilibrium configuration some internal cooperation strategies are unobservable. Such conclusion is not surprising, since the measured followers' trajectories at the steady states (which are straight lines) are not rich enough to reveal internal dynamics of the swarm. In this section, similar to Ref. [14], we introduce intruders as a possible *agent provocateur* to disrupt the adversarial swarm and provoke the swarm into more revealing behaviors. The agents in a non-cooperative swarm are assumed to treat an intruder as an obstacle with the interaction force between a vehicle and an intruder be expressed using an artificial potential V_r. Note that, we assume the adversarial swarm reacts to the intruder through a build-in obstacle avoidance algorithm. Such functionality may not be implemented in current autonomous swarms. However, given the rapid advancement of technology, it is reasonable to anticipated that obstacle avoidance algorithms such as those already implemented in autonomous driving cars may become available in future swarm applications.

For simplicity, we further assume that V_r is identical to potential V_I with the same parameters α, d_0, d_1 and K. In the simulation one intruder is initially at $(-100, -100)$ m and moves at a constant velocity of $(10, 2)$ m/s. Because the followers consider the intruder as a moving obstacle, they move around to avoid collision as the intruder penetrates the swarm; thus the steady state trajectory is perturbed to excite much richer dynamical behavior. Fig. 7 illustrates the

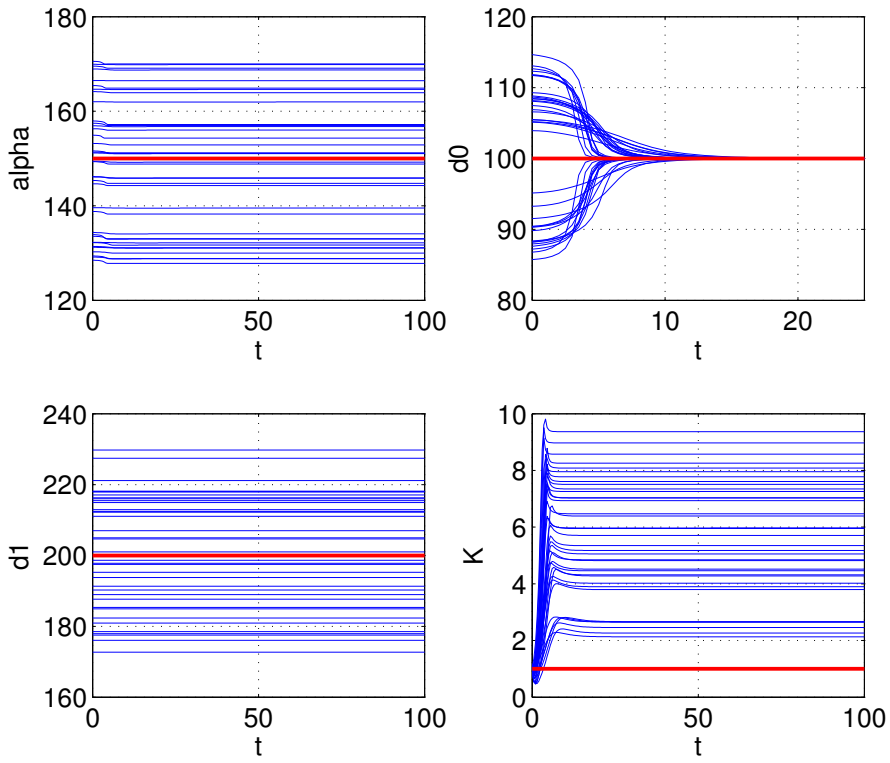

Fig. 6 UKF estimations of the parameters $p = [\alpha, d_0, d_1, K]$. Red solid lines are true values of the parameters. The dashed lines are UKF estimations.

trajectories of the perturbed swarm.

The empirical observability Gramian matrix of the intruder-perturbed swarm trajectory can be numerically computed using the same method as explained in the previous section. The minimum eigenvalue of the empirical observability Gramian is 0.4931; therefore, according to Proposition 1 the unobservability index with respect to all state variables and all unknown parameters is $1/\sqrt{0.4931} \approx 1.424$. With the intruder perturbing the stead state, the system becomes observable. Next, following the same process as in the case of steady state, we perform partial observability analysis on individual states. The results are shown in Table 3. Compared with Table 2, it is clear that introducing intruder significantly reduces the unobservability index of parameters α, d_1 and K by several magnitudes.

IV. Estimation of an Adversarial Swarm's Cooperation Strategy

Equipped with the results from partial observability analysis, we now address the problem of detecting the cooperating strategy of an adversarial swarm by estimating the leader states and parameters that define the internal interactive force among the agents in the swarm.

As shown in the previous section, when the steady state is perturbed by intruders, the entire system including all

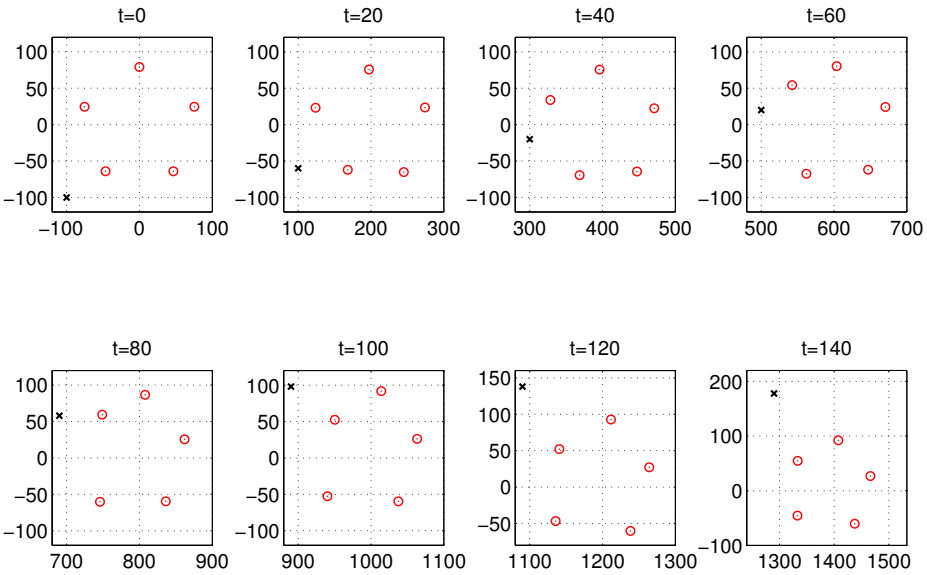

Fig. 7 Snapshots of positions of the swarm and intruder. Red ○: position of the follower; black ×: position of the intruder.

Table 3 Partial unobservability index of the swarm with intruder perturbation.

Estimation Variable (z)	Unobservability Index (ρ/ϵ)
Leader Position	2.231×10^{-1}
Leader Velocity	2.355×10^{-2}
Parameter α	1.958×10^{-1}
Parameter d_0	5.628×10^{-3}
Parameter d_1	1.099×10^{-2}
Parameter K	1.927×10^{-1}

parameters is fully observable. Therefore, standard filtering techniques for nonlinear estimation can potentially be applied to estimate the four parameters in the swarm system control architecture (α, d_0, d_1, K) and the virtual leader information, i.e., its initial position and velocity. However, when applying standard filtering techniques such as the UKF to estimate these parameters we have discovered that the estimates often fail to converge, see Fig. 8 for a typical performance of an UKF.

A couple of inherent challenges may contribute to the failure of the UKF in the estimation of the parameters. First, we have shown that all four parameters (α, d_0, d_1, K) and the virtual leader's position and velocity are observable based on the intruder perturbed trajectory; however, after the intruder passes through the region, the swarm will settle down to a new steady state, whose observability property can be fundamentally different to the intruder perturbed trajectory. To

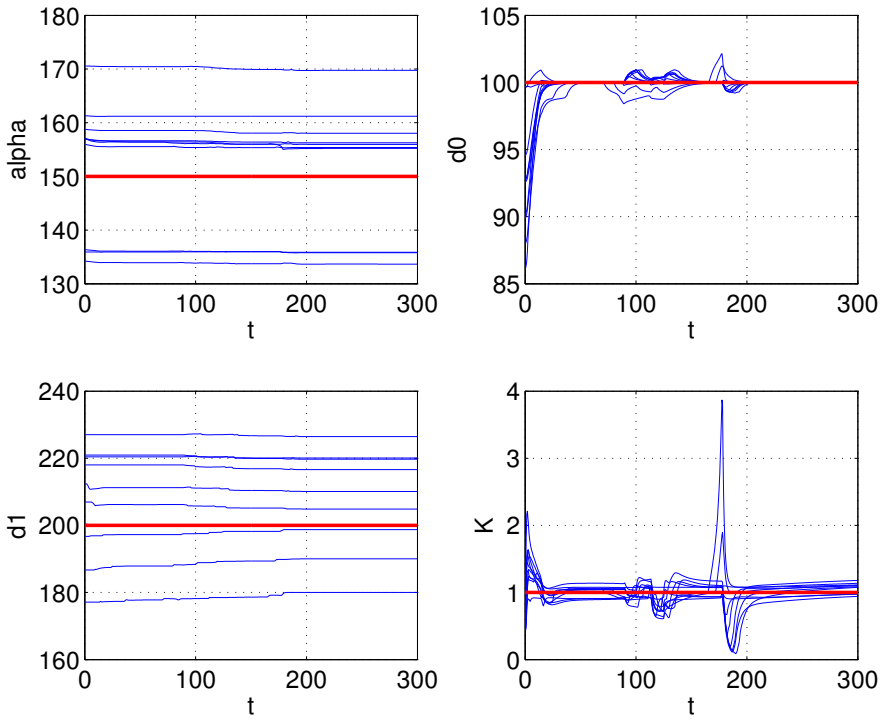

Fig. 8 Typical performance of an UKF. Red solid lines are true values of the parameters. The dashed lines are the estimates.

illustrate the change of unobservability indices, we computed the empirical observability Gramian matrices and the corresponding unobservability indices of parameters $[\alpha, d_0, d_1, K]$ over a sequence of moving observation windows of 100s long:

$$[t_k, t_k + 100],\ t_k = 10k,\ k = 0, 1, \ldots.$$

The results are shown in Fig. 9. It is clear that, except for d_0, which remains observable for all t, the observability of other three parameters subject to fundamental changes. As the intruder exits the swarm, parameters α, d_1 and K become unobservable. Such switch of observability introduces a fundamental challenge to UKF type of *sequential* estimation methods. If the filter has not converge before the swarm settles down to an unobservable steady state, all new measurements will not provide enough information for UKF to update its estimations, therefore, putting the convergence of the UKF in jeopardy. For complex and high dimensional nonlinear systems such as the adversarial swarm considered here, producing a fast convergent estimation (before the observability of the trajectory changes) by UKF is not straightforward; and may require a labor intensive process to tune UKF parameters.

Remark 1 *The concept of observability introduced in Section II-A clearly depends on the trajectory of the interest. Different trajectories of the same dynamical system may have different observability. Exemplified by the results in Figure*

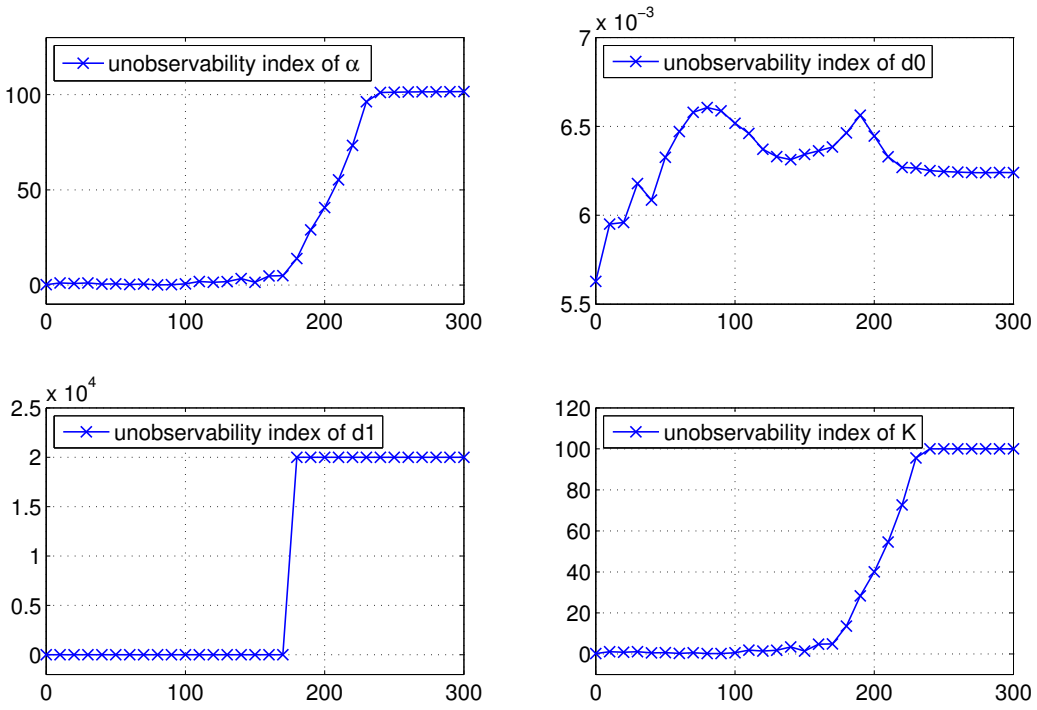

Fig. 9 Change of unobservability indices with respect to time.

9, we see that even different observation windows of the same trajectory can have completely different observability property.

The issue of UKF estimation is further complicated by another non-trivial challenge associated with parameter d_1, which represents the range limit of communication and/or range of influence among agents (see (14)). Parameter d_1 is fundamentally different from other parameters of the swarm. More specifically, if none of the relative distances between vehicles is equal to d_1, then a small perturbation around d_1 has no impact on the trajectory. Thus d_1 is not observable. Its value becomes observable only if the relative distance of at least one pair of vehicles passes across d_1. Therefore, d_1 is observable in a subset of parameter-state space. This subset is a surface that has zero measure. Such property makes the design of a convergent estimation algorithm a demanding task. To illustrate the challenge, we consider a simplified problem of estimating d_1 only with all other unknowns being fixed at their true values. Fig. 10 shows a typical result. The trajectory of the swarm is affected when the relative distances among the agents across the threshold defined by d_1. Therefore, the value of d_1 is locally distinguishable only in a zero measure subset of the state-parameter space, which causes the step-like behavior of the UKF estimation. The grey curves in the figure are the relative distances between agents. Note that the correction happens when the relative distance across the "fake" value assumed by the UKF. However, the filter fails to make correction when the relative distances across the true value of d_1.

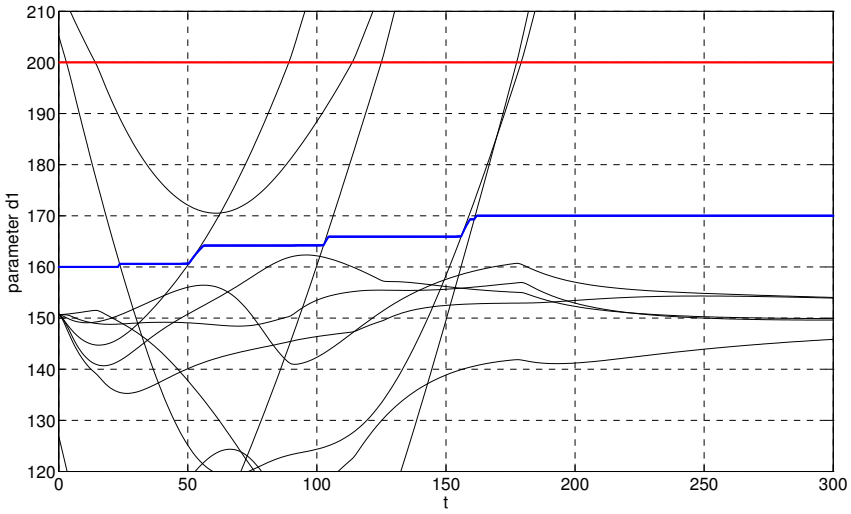

Fig. 10 UKF estimation of d_1, where all other parameters are given. Red solid line and blue dashed line are true and estimated values respectively. The grey lines are the relative distances between agents.

To overcome the inherent challenges of the considered estimation problem, we propose a two-stage algorithm using dynamical optimization.

Step 1. Based on the *unperturbed steady state* trajectory, construct the following dynamical optimization problem to estimate leader initial position, $x_l(0) \in R^2$, leader initial velocity, $\dot{x}_l(0) \in R^2$, and parameter d_0.

$$
\begin{cases}
\text{Find} & \hat{x}_l(0) \in R^2, \quad \hat{\dot{x}}_l(0) \in R^2, \text{ and } \hat{p} = [\hat{\alpha}, \hat{d}_0, \hat{d}_1, \hat{K}] \in \mathbb{R}^4 \text{ to} \\
\text{minimize} & J(\hat{x}_l(0), \hat{\dot{x}}_l(0), \hat{p}) = \log\left(1 + \int_0^{100} \|\hat{y}(t) - y(t)\|^2_{W_y} dt\right) \\
\text{subject to} & \dot{\hat{x}} = f(\hat{x}, \hat{p}, t), \\
& \hat{x}(0) = [\hat{x}_l^T(0), \hat{\dot{x}}_l^T(0), x_1^T(0), \dot{x}_1^T(0), \cdots, x_5^T(0), \dot{x}_5^T(0)]^T, \\
& \hat{y}(t) = [\hat{x}_1^T(t), \hat{\dot{x}}_1^T(t), \cdots, \hat{x}_5^T(t), \hat{\dot{x}}_5^T(t)]^T,
\end{cases}
\tag{19}
$$

where dynamics f is defined in (13)-(16), $y(t)$ is the measured followers' states defined in (17), and the weight matrix W_y is given in (18).

Problem (19) is an optimization problem with nonlinear dynamical constraint but finite dimensional decision variables. As shown in Section III-A, although the full system is not observable from the unperturbed steady state trajectory, the leader initial state and parameter d_0 are partially observable. Thus, Problem (19) is well-defined. Moreover, from the optimal solution, we obtain the estimates, $(\hat{x}_l(0), \hat{\dot{x}}_l(0), \hat{d}_0)$, of the true value of the leader initial state and parameter d_0. The estimation results are used in the next step. The other part of the optimal solution, i.e.,

$(\hat{\alpha}, \hat{d}_1, \hat{K})$, is discarded. Due to the nonlinear dynamical constraints, Problem (19) needs to be solved numerically. This can be done by incorporating an numerical integrator with a finite dimensional constraint optimization solver.

Step 2. Based on the intruder perturbed swarm trajectory, the following dynamical optimization is formulated for estimating parameters α, d_0 and K.

$$\begin{cases} \text{Find} & \hat{\alpha},\ \hat{d}_1,\ \text{and}\ \hat{K} & \text{to} \\ \text{minimize} & J(\hat{\alpha}, \hat{d}_1, \hat{K}) & = \log\left(1 + \displaystyle\int_0^{100} \|\hat{y}(t) - y(t)\|^2_{W_y}\, dt\right) \\ \text{subject to} & \dot{\hat{x}} & = f(\hat{x}, \hat{p}, t) \\ & \hat{x}(0) & = [\hat{x}_l^T(0), \hat{\dot{x}}_l^T(0), x_1^T(0), \dot{x}_1^T(0), \cdots, x_5^T(0), \dot{x}_5^T(0)]^T \\ & \hat{y}(t) & = [\hat{x}_1^T(t), \hat{\dot{x}}_1^T(t), \cdots, \hat{x}_5^T(t), \hat{\dot{x}}_5^T(t)]^T \end{cases} \tag{20}$$

where dynamics f is defined in (13)-(16), $\hat{p} = [\hat{\alpha}, \hat{d}_0, \hat{d}_1, \hat{K}]$, $y(t)$ is the measured followers' states defined in (17), and the weight matrix W_y is given in (18). Note that in this optimization problem, the decision variables are $\hat{\alpha}$, $\hat{d}_1$, and $\hat{K}$. The leader initial state and parameter d_0 are fixed at their estimated values, i.e., $(\hat{x}_l^T(0), \hat{\dot{x}}_l^T(0), \hat{d}_0)$, from Step 1.

Remark 2 *Both dynamical optimization problems (19) and (20) process entire measured trajectory at once; thus circumvents some challenges associate with UKF type of sequential estimation tools. The partial observability of parameters depends on the time window. Step 1 can be applied to find the observable parameters only, without the help of the intruder. Its computation can be carried out before the intruder enters the region of action. However, Step 2 must be done using the data collected during the time window when the intruder passes through the swarm.*

The optimization problems (19) and (20) are solved numerically using nonlinear programming solver SNOPT. The estimation errors of the virtual leader state and the parameters in Step 1 are reported in Table 4. These errors are averaged over 10 runs from random initial guesses range from ±50% of the true values. Average runtime in MATLAB is 247 seconds on a MacBook Pro with 2.3GHz i7 cpu and 8 GB memory. Although the system is not fully observable, the leader initial states and parameter d_0 can indeed be estimated with high accuracy as predicted in partial observability analysis. Furthermore, the optimal cost is in the order of 10^{-8} indicating that different cooperation parameters α, d_1 and K can generate identical follower trajectories; thus α, d_1 and K cannot be observable from the considered steady state.

Numerical estimations, $(\hat{x}_l(0), \hat{\dot{x}}_l(0), \hat{d}_0)$, from Step 1 are used to construct optimization problem (20) in Step 2, which is again solved numerically using SNOPT. From the optimal estimation errors reported in Table 5, it is clear that all three parameters, α, d_1 and K, have been identified. These errors are averaged over 10 runs from random initial guesses within ±50% of the true values. Average runtime in MATLAB is 398 seconds on a MacBook Pro with 2.3GHz

Table 4 Estimation errors of Step 1. The errors are averaged over 10 runs from random initial guesses. The relative errors are scaled by the corresponding true values.

estimation variable (z)	estimation error	relative estimation error
$x_l(0) = (0, 0)$	2.395×10^{-4}	N/A
$\dot{x}_l(0) = (10, 0)$	2.991×10^{-6}	2.991×10^{-7}
$\alpha = 150$	21.76	0.1451
$d_0 = 100$	2.967×10^{-5}	2.967×10^{-7}
$d_1 = 200$	19.104	9.552×10^{-2}
$K = 1$	7.190	7.190

i7 cpu and 8 GB memory. It is worth pointing out that the discontinuous parameter d_1 is estimated with higher accuracy than the other two parameters α and K, which is consistent to the partial unobservability indices reported in Table 3.

Table 5 Estimation errors of Step 2. The errors are averaged over 10 runs from random initial guesses. The relative errors are scaled by the corresponding true values.

estimation variable (z)	estimation error	relative estimation error
$\alpha = 150$	1.117×10^{-2}	7.447×10^{-5}
$d_1 = 200$	2.915×10^{-4}	1.458×10^{-6}
$K = 1$	6.610×10^{-5}	6.610×10^{-5}

Remark 3 *Instead of the proposed two-step algorithm, it is possible to formulate a single dynamical optimization problem to estimate all variables of interest, i.e., adding* $\hat{p} = [\hat{\alpha}, \hat{d}_0, \hat{d}_1, \hat{K}]$ *as decision variables into Problem (20). However, based on our numerical tests, the proposed two-step algorithm is more efficient in terms of runtime and robustness to the initial guess. Comparing with the single step optimization that involves all unknowns, the proposed two-step algorithm based on observability analysis effectively reduces the dimension of the dynamical optimization problem, thus improves the numerical performance.*

Remark 4 *It is worth pointing out that computational cost in the proposed two-step estimation algorithm grows rapidly as the size of the swarm increases. Such phenomenon appears also in sequential estimation techniques including UKF and extended Kalman filter. How to design computationally efficient estimation algorithms for high dimensional systems, for example, adversarial swarms with a large number of agents, is an important subject of ongoing research. In particular, distributed and parallel computational tools that explicitly explore partial observability of nonlinear system have great potential to lift the curse of dimensionality. However, this is beyond the scope of this paper.*

V. Conclusions

This paper applies the concept of partial observability and its associated computational tools for analyzing the observability of the internal cooperating strategy of an adversarial swarm model. This new approach allows quantitative observability analysis on individual state even when the whole system is not observable in traditional sense. Our simulations reveal that when an adversarial swarm is at a steady state that is not fully observable, some parameters that define the internal cooperating strategy can still be partially observable; thus be accurately estimated while the overall system is unobservable. When intruder perturbation is introduced, the computation of partial observability indices clearly shows the dependences of observability on the swarm's trajectory, as well as the time window during which the swarm reacts to the intruder. To address convergence issues of UKF for estimating parameters that are observable on a zero measure subset, we developed a two-step estimation algorithm based on dynamical optimization. The proposed algorithm utilizes the concept of partial observability to circumvent some fundamental challenges associated with UKF types of sequential estimation tools. The results in this paper provide useful tools for further study on the estimation of adversarial swarms in more realistic scenarios, for example large swarms with unknown number of agents, swarms with different potential functions, and non-potential based swarm models.

VI. Appendix

A. Appendix

Proof of Proposition 1

Given a nominal trajectory of (4) with initial state $x(0)$. Given a variation $\delta x(0)$. Let $y(t)$ and $\hat{y}(t)$ be the corresponding outputs. Then

$$\hat{y}(t) - y(t) = Ce^{At}\delta x(0)$$

It is easy to verify

$$\begin{aligned} ||\hat{y}(\cdot) - y(\cdot)||_{L^2} &= \int_0^T \delta x(0)^T e^{A^T\tau} C^T C e^{A\tau} \delta x(0) d\tau \\ &= \delta x(0)^T G \delta x(0). \end{aligned}$$

The projection of $\mathcal{E}$ to the initial state space is an ellipsoid in $\mathbb{R}^{n_x}$ centered around $x(0)$

$$\mathcal{P}(\mathcal{E}) = \left\{ x(0) + \delta x(0) \,\middle|\, \delta x(0)^T G \delta x(0) \le \epsilon^2 \right\} \tag{21}$$

Let $\lambda_{\min}$ be the smallest eigenvalue of G with an associated eigvenvector $x_{\min}$ on the surface

$$x_{\min}^T G x_{\min} = \epsilon^2 \tag{22}$$

Then $x_{\min}$ is the major principle axis of the ellipsoid (21). Denote

$$\rho = ||x_{\min}||_2,$$

then ρ is the radius of $\mathcal{P}(\mathcal{E})$, i.e.,

$$\rho = \max_{x(0)+\delta x(0)\in\mathcal{P}(\mathcal{E})} ||\delta x(0)||_2$$

From (22), we have

$$\epsilon^2 = \lambda_{\min}||x_{\min}||_2^2$$

Thus the unobservability index is $\rho/\epsilon = 1/\sqrt{\lambda_{\min}}$.

ACKNOWLEDGMENT

This work was supported in part by Office of Naval Research under grants N0001417WX01098 and N0001419WX00155.

References

[1] N. Leonard and E. Fiorelli, Virtual leaders, artificial potentials and coordinated control of groups, Proceedings of the 40th IEEE Conference on Decision and Control, vol. 3, pp. 2968–2973, 2001.
DOI: 10.1109/CDC.2001.980728

[2] P. Ogren, E. Fiorelli, and N. Leonard, Cooperative control of mobile sensor networks: Adaptive gradient climbing in a distributed environment, IEEE Transactions on Automatic Control, vol. 49, no. 8, pp 1292–1302, 2004.
DOI: 10.1109/TAC.2004.832203

[3] A. Jadbabaie, J Lin, and A. S. Morse, Coordination of groups of mobile autonomous agents using nearest neighbor rules, IEEE Transactions on Automatic Control, vol. 48, no. 6, pp. 988–1001, 2003.
DOI: 10.1109/TAC.2003.812781

[4] K. Szwaykowska, C. Heckman, L. Mier-y-Teran-Romero, and I. Schwartz, Pattern-acquisition in finite, heterogenous, delay-coupled swarms, arXiv preprint, arXiv:1502.07978. 2015.

[5] T. Chung, M. Clement, M. Day, K. Jones, D. Davis, and M. Jones, Live-fly, Large-scale field experimentation for large numbers of fixed-wing UAVs, IEEE International Conference on Robotics and Automation (ICRA), Sweden, 2016.
DOI: 10.1109/ICRA.2016.7487257

[6] A. A. Paranjape, S. J. Chung, K. Kim, and D. H. Shim, Robotic herding of a flock of birds using an unmanned aerial vehicle, IEEE Transactions on Robotics, vol. 34, no. 4, pp. 901–915, 2018.
DOI: 10.1109/TRO.2018.2853610

[7] C. Walton, P. Lambrianides, I. Kaminer, J.O. Royset, and Q. Gong, Optimal motion planning in rapid-fire combat situations with attacker uncertainty, Naval Research Logistics, vol. 65, no. 2, pp. 101–119, 2018.
DOI: 10.1002/nav.21790

[8] T. Kailath, Linear Systems, Englewood Cliffs, NJ, USA: Prentice- Hall, 1980.

[9] S. Diopand and M. Filess, Nonlinear observability, identifiability, and persistent trajectories, in Proc. 30th IEEE Conf. Decision and Control, vol. 1, pp. 714-719, 1991
DOI: 10.1109/CDC.1991.261405

[10] R. Hermann and A. Krener, Nonlinear controllability and observability, IEEE Transactions on automatic control, vol. 22, no. 5, pp. 728-740, 1977.
DOI: 10.1109/TAC.1977.1101601

[11] JP. Gauthier and IAK. Kupka,Observability and observers for nonlinear systems, SIAM journal on control and optimization, vol 32, no 4, pp. 975–994, 1994.
DOI: 10.1137/S0363012991221791

[12] X. Xia and W. Gao. Nonlinear observer design by observer error linearization, SIAM Journal on Control and Optimization vol. 27, no. 1, pp. 199-216, 1989.
DOI: 10.1137/0327011

[13] G. Zheng, B. Driss, and JP. Barbot. Single output-dependent observability normal form, SIAM Journal on Control and Optimization, vol. 46, no. 6, pp. 2242-2255, 2007. DOI: 10.1137/050627137

[14] H. Park, Q. Gong, W. Kang, C. Walton, and I. Kaminer, Observability analysis of an adversarial swarm's cooperation strategy, the 14th IEEE International Conference on Control and Automation (ICCA), Anchorage, Alaska, June, 2018.
DOI: 10.1109/ICCA.2018.8444217

[15] A. Krener and K. Ide, Measures of unobservability, Proceedings of the 48th IEEE Conference on Decision and Control, pp. 6401–6406, 2009.
DOI: 10.1109/CDC.2009.5400067

[16] W. Kang and L. Xu, A quantitative measure of observability and controllability. Proceedings of the 48th IEEE Conference on Decision and Control, pp. 6413–6418, 2009.
DOI: 10.1109/CDC.2009.5399945

[17] N. Powel and K. Morgansen, Empirical observability Gramian rank condition for weak observability of nonlinear systems with control, IEEE 54th Annual Conference on Decision and Control, pp. 6342–6348, 2015.
DOI: 10.1109/CDC.2015.7403218

[18] W. Kang and L. Xu, Computational analysis of control systems using dynamic optimization, arXiv preprint, arXiv:0906.0215, 2009.

[19] J. Qi, K. Sun, and W. Kang, Optimal PMU placement for power system dynamic state estimation by using empirical observability Gramian, IEEE Trans. Power Systems, Vol. 30, No. 4, pp 2041-2054, 2015.
DOI: 10.1109/TPWRS.2014.2356797

[20] J. Qi, K. Sun, and W. Kang, Adaptive optimal PU placement based on empirical observability Gramian, Proceedings of IFAC NOLCOS 2016, IFAC-PapersOnLine 49-18, pp. 482-487, 2016.
DOI: 10.1016/j.ifacol.2016.10.211

[21] S. Julier and J. Uhlmann, A new extension of the Kalman filter to nonlinear systems, International Symposium on Aerospace/Defense Sensing, Simuluation, and Controls, vol. 3, no. 26, pp. 182–193. 1997.
DOI: 10.1117/12.280797